

# Spin Wave Lifetimes Throughout the Brillouin Zone

S.P. Bayrakci,<sup>1</sup> T. Keller,<sup>1,2</sup> K. Habicht,<sup>3</sup> and B. Keimer<sup>1</sup>

<sup>1</sup>Max-Planck-Institut für Festkörperforschung, Heisenbergstr. 1, 70569 Stuttgart, Germany

<sup>2</sup>ZWE FRMII, Technische Universität München, Lichtenbergstr. 1, 85748 Garching, Germany

<sup>3</sup>Hahn-Meitner-Institut, Glienickerstr. 100, 14109 Berlin, Germany

To whom correspondence should be addressed; E-mail: bayrakci@fkf.mpg.de.

**We use a neutron spin-echo method with eV resolution to determine the lifetimes of spin waves in the prototypical antiferromagnet  $\text{MnF}_2$  over the entire Brillouin zone. A theory based on the interaction of magnons with longitudinal spin fluctuations provides an excellent, parameter-free description of the data, except at the lowest momenta and temperatures. This is surprising, given the prominence of alternative theories based on magnon-magnon interactions in the literature. The results and technique open up a new avenue for the investigation of fundamental concepts in magnetism. The technique also allows measurement of the lifetimes of other elementary excitations (such as lattice vibrations) throughout the Brillouin zone.**

The concept of elementary excitations is one of the basic pillars of the theory of solids. In the low-temperature, long-wavelength limit, such excitations do not interact and have an infinite lifetime. For nonzero temperatures and momenta, the lifetimes of elementary excitations are generally limited by collisions with other excitations, with important consequences for the macroscopic properties of solids. For instance, the thermal expansion of solids can be understood as a consequence of collisions between lattice vibrations (phonons). Because of their comparatively simple Hamiltonians, magnetically-ordered states are excellent testing grounds for theories of elementary excitations and their interactions. Despite this, the damping of spin waves (magnons) in antiferromagnets has remained an open problem for four decades. Theoretical calculations of magnon lifetimes have been carried out since the 1960's, with intensive development occurring on several fronts in the early 1970's. However, these activities ground to a halt by the mid-1970's due to the lack of appropriate experimental data, namely, from momentum-resolved measurements with sufficient energy resolution. The only low-temperature data available were taken with  $q = 0$ , in antiferromagnetic resonance (AFMR) and parallel pumping measurements [1, 2]. Because of the limited energy resolution, momentum-resolved data from neutron spectroscopy [3], on the other hand, were confined to the critical regime extremely close to the Néel temperature ( $T_N$ ), where most theories do not apply. Until recently, no other experimental techniques were available which permitted high-resolution measurements of excitation lifetimes at low temperatures over the whole Brillouin zone. We report on a new neutron spectroscopy method with  $\mu\text{eV}$  resolution which is used to measure spin wave (magnon) lifetimes in the prototypical antiferromagnet  $\text{MnF}_2$  over the temperature range from  $0.04 - 0.6 T_N$ . The results subject long-standing theoretical predictions to a first experimental test and hold promise as a novel probe of elementary excitations in quantum magnets. The technique is also widely applicable to other elementary excitations such as phonons and crystal field excitations.

The determination of magnon lifetimes at low temperatures requires an energy resolution in the eV range, about two orders of magnitude better than that achievable by standard neutron triple-axis spectroscopy (TAS). We have obtained the requisite gain in resolution by manipulating the Larmor phase of the neutron spin with magnetic fields. The TRISP spectrometer (Fig. 1A) weds the capability of TAS of accessing collective excitations throughout the Brillouin zone to the extremely high energy resolution of neutron spin-echo spectroscopy[5]. As in typical spin-polarized triple-axis spectrometry, the neutrons impinging upon the sample are polarized, and the polarization of neutrons scattered from the sample is measured. On TRISP, this is accomplished through the use of a polarizing neutron guide and a transmission polarizer, respectively. However, in analogy to neutron spin-echo spectrometry, the TRISP spectrometer also includes regions of effectively constant magnetic field which are produced by pairs of radio-frequency (RF) resonance coils inserted symmetrically 1) between the monochromator and sample and 2) between the sample and the analyzer [6]. The RF frequencies in the coils are tuned such that each detected neutron that creates an excitation lying on the magnon dispersion curve has the same net Larmor phase after traversing the two spin-echo arms, independent of small variations in the wave vector of the excitation. The neutron spin polarization determined at the detector is then a measure of the linewidth (inverse lifetime) of the magnon. In this way, the measured linewidth is decoupled (to first order) from the spread in energy of the neutrons incident on the sample, which is responsible for the instrumental resolution in TAS. (For a detailed description of the technique, see the Materials and Methods section.)

We chose the antiferromagnet  $\text{MnF}_2$  for the experiment, as its magnetic ground state and excitations have been investigated extensively. The lattice structure and magnetic ordering of  $\text{MnF}_2$  are shown in Fig. 1B.  $\text{MnF}_2$  has the body-centered tetragonal structure, with  $a = b = 4.8736 \text{ \AA}$  and  $c = 3.2998 \text{ \AA}$ . The  $\text{Mn}^{2+}$  ions have spin  $S = 5/2$ , and the spin in the center of the unit cell is oriented antiparallel to those at the corners. The strongest magnetic interaction is

between second-nearest-neighbor  $\text{Mn}^{2+}$  spins (corner and center spins) and is antiferromagnetic [7]. A weaker, ferromagnetic interaction exists between nearest-neighbor spins (along the  $c$ -axis). A relatively strong uniaxial anisotropy which is predominantly the result of dipole-dipole interactions [8, 9] causes the spins to align along the  $c$ -axis.  $T_N$  is 67.6 K. The slope of the magnon dispersion is required to set the tilt angles of the RF coils and to determine the non-intrinsic contribution to the data (see Materials and Methods). During the experiment, the spin-wave dispersion was therefore measured at each temperature at which linewidth data was taken; a partial data set is shown in Fig. 1C.

Fig. 2 shows raw polarization data as a function of the spin-echo time  $\tau$ . The spin-echo time is proportional to the frequency in the RF coils and the distance between the coils, and also depends on the neutron wavelength. In a neutron spin-echo experiment, the dependence of the measured polarization on  $\tau$  corresponds to the Fourier transform of the scattering function as a function of energy. The data in Fig. 2 are described well by an exponential decay, which indicates that the spectral function which characterizes the magnon linewidth is a Lorentzian in energy. The difference in linewidth (half-width at half maximum, or HWHM) between the upper two and lower two data sets is in each case only  $\sim 3$  eV, but it can be resolved clearly. The upper pair of data sets represents a difference in  $q$  of 0.05 r.l.u. at 15 K [10]. For comparison, the HWHM of the corresponding TAS scans of the lower two magnons in Fig. 2, taken with fixed final neutron wave vector  $k_f = 1.7 \text{ \AA}^{-1}$ , is approximately 100 eV.

The raw data were then corrected for instrumental and non-intrinsic effects [11]. Figs. 3 and 4 show the intrinsic magnon linewidth as a function of momentum  $q$  and temperature  $T$ , respectively. The linewidth generally increases with increasing  $q$  and  $T$ , due to the increasing likelihood of collisions with other excitations. However, Fig. 3 also shows that the linewidth deviates from this general trend and exhibits peaks as a function of  $q$  close to the center and the boundary of the antiferromagnetic Brillouin zone. The low- $q$  peak is already present at 3

K, the lowest temperature covered by this experiment, and it evolves weakly with increasing temperature. This behavior is not described by the dominant magnon relaxation mechanisms for which quantitative predictions are available; possible origins will be discussed below. In order to facilitate comparison with these predictions, we have treated the 3 K linewidth data as a temperature-independent contribution and subtracted it from the higher-temperature data. The results are shown in the main panels of Figs. 3 and 4.

The intrinsic relaxation channel for magnons that has received by far the most attention in the literature is magnon-magnon scattering. In an “ $n$ -magnon” scattering event, a magnon (here, one excited by an incoming neutron) scatters off ( $n=2-1$ ) thermally excited magnons, producing  $n=2$  scattered magnons which are in thermal equilibrium with the sample. In the absence of defects and external magnetic fields, the lowest-order interaction which limits the magnon lifetime is 4-magnon scattering. Unfortunately, a comprehensive survey of the literature revealed very few theoretical predictions appropriate for comparison with our data, despite the existence of considerable work on 4- and 6-magnon interactions. This is either because the calculations employed approximations valid only in high magnetic fields (for the purpose of comparison with AFMR data), or because strict inequalities that define the range of applicability of the theoretical results are extremely difficult to satisfy experimentally. An analytical expression was given by Harris *et al.* [12], who evaluated the contribution to the linewidth from 4-magnon scattering processes analytically for the case of single-ion anisotropy with  $\alpha = 0$  [13]. The corresponding result is shown in the bottom trace of Fig. 4. At low temperatures, the temperature dependence of the data is considerably weaker than that predicted by this theoretical result for  $\alpha = 0$ . The best agreement of the magnitude occurs at 40 K, where the experimental result is 30% larger than the theoretical. Predictions for an anisotropy gap of dipolar origin, which would be more appropriate for  $\text{MnF}_2$ , are not available.

An additional relaxation channel, in which magnons are scattered by thermally-excited lon-

itudinal spin fluctuations, was considered by Stinchcombe and coworkers [14, 15]. The curves in Figs. 3 and 4 are based on this mechanism. (For  $\eta = 0$ , where the contribution of this relaxation is identically zero, we have shown the prediction of the 4-magnon relaxation model, as discussed above.) For the larger- $\eta$  data, the linewidth far from  $T_N$  is given approximately by

$$\eta (HW_{HM}) = \frac{R_0^0}{4 R_0^2} \eta \frac{(1 + \eta)^2}{[1 + (1 + \eta)J(0)R_0^0]}; \quad (1)$$

where  $\eta$  is the magnon energy,  $\eta = 2 \eta a$ ,  $a = 2.969 \text{ \AA}^2$ ,  $a^3 = 5.864 \text{ \AA}^3$ , and  $\eta = 1/k_B T$ , with  $k_B$  the Boltzmann constant [15]. The anisotropy parameter  $\eta$  is equal to 0.0184. The exchange parameter  $J(0) = 6.02 \text{ meV}$  includes both first- and second-nearest neighbor exchange interactions. The parameters  $R_0$  and  $R_0^0$ , which are both temperature-dependent, can each be evaluated using either experimental data or results from mean-field theory [15], leading to considerable differences in the magnitude of the calculated linewidth and in its variation with temperature. In determining  $R_0$ , we used experimental data for the staggered magnetization [16]. Calculation of  $R_0$  from the Brillouin function produces linewidth values which agree at the lowest temperatures and begin to deviate with increasing temperature: at 40 K, the calculated linewidth is 11% smaller. For  $R_0^0$ , we used the derivative of the Brillouin function. Calculation of  $R_0^0$  instead from experimental data for the parallel magnetic susceptibility [17] produces linewidth results which are 40% larger at 15 K and 30% smaller at 40 K.

Given the prominence of the magnon-magnon scattering channel in the literature, the excellent agreement between this model calculation and the experimental data is surprising. The dominance of the relaxation by longitudinal fluctuations is, however, consistent with arguments by Reinecke and Stinchcombe, who estimated that the contribution to the linewidth from 4-magnon scattering is only  $1/z$  of the magnitude of the above term [18]. Here,  $z$  is the number of neighbors which experience the strongest exchange interaction;  $z = 8$  for  $\text{MnF}_2$ , for which case  $z$  is the number of next-nearest neighbors [19]. As the analytical expression on which the

curves in Figs. 3 and 4 are based is valid only at low  $q_x$  deviation from the data at larger  $q_x$  is not unexpected. The general expression for the linewidth resulting from scattering by longitudinal spin fluctuations [14, 15] should be evaluated numerically at high  $q_x$  to see if the peak as a function of  $q_x$  can be reproduced [33, 34].

An explanation of the peak centered at  $q_x = 0 \pm 1$  r.l.u. (inset in Fig. 3) requires a different mechanism [20]. An additional potential source of linewidth is the hyperfine interaction, which gives rise to the scattering of electronic magnons from nuclear spin fluctuations [21]. The contribution from the hyperfine interaction would only be weakly temperature dependent, because the nuclear spin system is already highly disordered thermally at 3 K. 4-magnon scattering terms in which one electronic and one nuclear magnon interact have indeed been shown to generate maxima in the linewidth at nonzero  $q_x$  but estimates of the amplitude of this contribution are at least an order of magnitude smaller than the observed effect [21]. The crossing of magnon and TA phonon modes at  $q_x = 0.04$  r.l.u. may also contribute to the peak [22, 23, 24]. An additional relaxation mechanism which must be considered as a possible source of linewidth is that of magnon-phonon scattering. Experimental estimates of the linewidth due to magnon-phonon relaxation in  $\text{MnF}_2$  in zero field range over three orders of magnitude, but again appear too small to explain the observed peak [25, 26, 27]. A theoretical estimate of the spin-lattice relaxation time (which should be of the same order of magnitude as the magnon-phonon relaxation times) corresponds to a linewidth of  $\sim 0.5$  eV at 25 K in  $\text{MnF}_2$  [28, 29]. In this theory, the magnon-phonon interaction arises from the phonon modulation of the exchange interaction, and is dominated by 2-magnon-1-phonon processes. The result varies as  $T^5$ , which corresponds to a linewidth of 1 eV at 30 K and 5 eV at 40 K. The maximum potential contribution to our data would then be  $\sim 60\%$  of the linewidth at  $q_x = 0$  and 40 K. Other mechanisms which may contribute to the presence of this peak include 2- and 3-magnon non-momentum-conserving processes which originate from scattering from defects [30, 31, 21]. The linewidth originating

from the latter process is peaked at intermediate  $q$ . Using parameters derived from comparison with data on  $\text{RbMnF}_3$ , its contribution in  $\text{MnF}_2$  can be estimated to be two orders of magnitude smaller than the data [31].

The challenge to theory posed by the temperature- and momentum-dependent peaks in the magnon linewidth in  $\text{MnF}_2$  should stimulate new activity in the field of spin wave decay mechanisms. High-resolution lifetime measurements over the full Brillouin zone in a relatively simple antiferromagnet such as  $\text{MnF}_2$  permit detailed evaluation of proposed processes, which should provide a basis for addressing such interactions in more complex magnetic systems.

## References and Notes

- [1] J.P. Kotthaus, V. Jaccarino, *Phys. Lett. A* **42**, 361 (1973).
- [2] J. Barak, S.M. Rezende, A.R. King, V. Jaccarino, *Phys. Rev. B* **21**, 3015 (1980).
- [3] M.P. Schulhof, R. Nathans, P. Heller, A. Linz, *Phys. Rev. B* **4**, 2254 (1971).
- [4] F. Mezei, *Z. Phys.* **255**, 146 (1972).
- [5] T. Keller *et al.*, *Appl. Phys. A* **74**, S332 (2002).
- [6] R. Golub, R. Gähler, *Phys. Lett. A* **123**, 43 (1987).
- [7] A. Okazaki, K.C. Turberfield, R.W. Stevenson, *Phys. Lett.* **8**, 9 (1964).
- [8] F. Keffer, *Phys. Rev.* **87**, 608 (1952).
- [9] J. Barak, V. Jaccarino, S.M. Rezende, *J. Magn. Magn. Mater.* **9**, 323 (1978).
- [10] We use a notation in which the momentum  $Q$  transferred by the neutron is  $Q = q + G$ , where  $q$  is the momentum transfer within the Brillouin zone centered at the reciprocal lattice vector  $G$ . These quantities are expressed in reciprocal lattice units (r.l.u.). For instance,  $Q = (HKL)$ , with  $Q_a = H$  ( $2 = a$ ), and  $q = (hkl)$ , with  $q_c = l$  ( $2 = c$ ).
- [11] Materials and methods are available as supporting material on *Science Online*.
- [12] A.B. Harris, D. Kumar, B.I. Halperin, P.C. Hohenberg, *Phys. Rev. B* **3**, 961 (1971).
- [13] The conditions for application of the results of Harris *et al.* in various intervals of temperature and energy are quite restrictive due to the presence of strict inequalities, and the resulting analytical expressions for the linewidth are valid only in extremely limited regions,

if at all. Here, we have treated these conditions as if they involved simple inequalities, and have plotted the four solutions which apply to different temperature regions together.

- [14] M.G. Cottam, R.B. Stinchcombe, *J. Phys. C: Solid State Phys.* **3**, 2305 (1971).
- [15] R.B. Stinchcombe, T.L. Reinecke, *Phys. Rev. B* **9**, 3786 (1974).
- [16] V. Jaccarino in *Magnetism*, G.T. Rado, H. Suhl, Eds. (Academic Press, New York, 1965), vol. 2A, pp. 307-355.
- [17] S. Foner in *Magnetism*, G.T. Rado, H. Suhl, Eds. (Academic Press, New York, 1963), vol. 1, pp. 383-447.
- [18] T.L. Reinecke, R.B. Stinchcombe, *Phys. Rev. B* **21**, 5198 (1980).
- [19] In contrast, in earlier work Cottam and Stinchcombe suggest that in the general case, the linewidth contribution from 4-magnon scattering dominates at low temperatures [14].
- [20] The effect of the curvature of the magnon dispersion on the spin-echo resolution is largest at  $q = 0$ , and largest at low temperature, where the spin-wave stiffness is strongest. Thus, curvature not properly taken into account in the analytical correction calculation would produce an apparent linewidth. However, this spurious effect would be peaked at  $q = 0$ , and is therefore unlikely to be responsible for the observed peak.
- [21] R.B. Woolsey, R.M. White, *Int. J. Magn.* **2**, 51 (1972).
- [22] R.L. Melcher, *Phys. Rev. B* **2**, 733 (1970).
- [23] C.A. Rotter, cited by H.G. Smith, N. Wakabayashi in *Dynamics of Solids and Liquids by Neutron Scattering*, S.W. Lovesey, Ed. (Springer-Verlag, Berlin, 1977), p. 93.
- [24] H. Montgomery, A.P. Cracknell, *J. Phys. C: Solid State Phys.* **6**, 3156 (1973).

- [25] L.D. Rotter, W.D. Dennis, W.M. Yen, *Phys. Rev. B* **42**, 720 (1990).
- [26] G.J. Jongerden, A.F.M. Arts, J.I. Dijkhuis, H.W. de Wijn, *Phys. Rev. B* **40**, 9435 (1989).
- [27] L.D. Rotter, W. Grill, W.M. Dennis, *J. Lumin.* **45**, 130 (1990).
- [28] M.G. Cottam, *J. Phys. C: Solid State Phys.* **7**, 2919 (1974).
- [29] A.Y. Wu, R.J. Sladek, *Phys. Rev. B* **25**, 5230 (1982).
- [30] R. Loudon, P. Pincus, *Phys. Rev.* **132**, 673 (1963).
- [31] R.B. Woolsey, thesis, Stanford University (1970).
- [32] R.M. White, R. Freedman, R.B. Woolsey, *Phys. Rev. B* **10**, 1039 (1974).
- [33] A suggestion of non-monotonic behavior in the linewidth as a function of  $q$  is contained in Ref. [14]. For the case in which the anisotropy takes the form of an anisotropy field  $H_A$ , the linewidth peaks at an intermediate value of  $q$  and then declines as it approaches the Brillouin zone boundary at  $q = 0.5$  r.l.u. However, the estimated value of  $q$  at which the peak occurs would be only  $0.008$  r.l.u. for  $MnF_2$ . The behavior of the linewidth at large  $q$  for the case of anisotropic exchange was not evaluated.
- [34] Woolsey and White [21] predict a peak as a function of  $q$  in  $MnF_2$  for the linewidth due to a 4-magnon scattering process in a relatively small magnetic field between 2 and 3 K. The peak becomes less pronounced and shifts to higher  $q$  as the temperature increases to 3 K (from 0.30 r.l.u. at 2 K to 0.37 r.l.u. at 3 K). At a slightly higher field, only a simple maximum is present between 4 and 10 K for a 4-magnon scattering process [31]. The authors did not incorporate anisotropy in their calculations; later work by the same authors showed that the inclusion of anisotropy results in a decrease in the calculated linewidth of roughly an order of magnitude for  $q = 0$  in a large magnetic field [32].

[35] We would like to express our thanks to G. Schmidt of the Crystal Growth Facility of the Cornell Center for Materials Research for the loan of a  $\text{MnF}_2$  crystal of excellent quality, R. Henes and J. Major for the gamma-ray diffractometry measurements, J. Peters for cryogenic assistance, G. Khaliullin and R.K. Kremer for illuminating discussions, P. Aynajian for participation in some of the calibration measurements, and R. Noack for technical assistance.

### **Supporting Online Material**

[www.sciencemag.org](http://www.sciencemag.org)

Materials and Methods

Fig. S1

References

### **Figures**

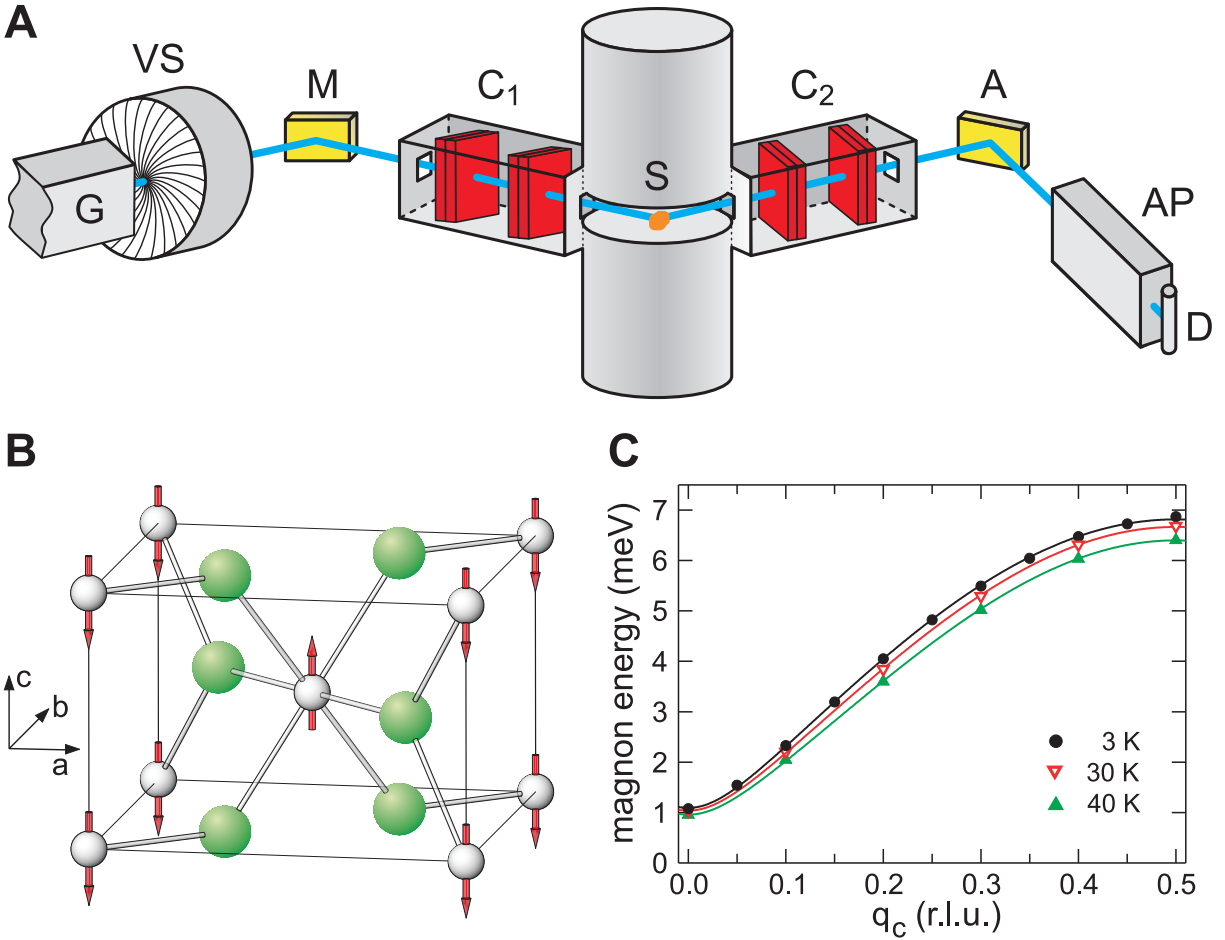


Figure 1: **(A)** A diagram of the spectrometer TRISP at the FRM-II. G denotes the polarizing guide and AP the transmission polarizer; M and A are the monochromator and analyzer, as in TAS. S is the sample and D the detector; VS indicates the velocity selector. The resonance coil pairs ( $C_1$  and  $C_2$ ) are shown in red, and the mu-metal shielding boxes which enclose them in gray. The blue ray represents the path of the neutrons through the spectrometer, from left to right on the diagram. **(B)** The crystal and magnetic structure of  $\text{MnF}_2$ . The gray (smaller) spheres represent  $\text{Mn}^{2+}$  ions and the green (larger) spheres the  $\text{F}^-$  ions. The arrows indicate the relative directions of the  $\text{Mn}^{2+}$  spins on the respective sublattices. **(C)** The magnon dispersion along the  $q_c$  direction at three selected temperatures at and below 40 K. The data was taken on TRISP during the course of the linewidth measurements. The curves show the results of fits based on the same spin-wave result used by Okazaki *et al.* [7], in which the anisotropy is expressed by a single-ion form, and in which the interactions of up to third-nearest neighbors are taken into account.

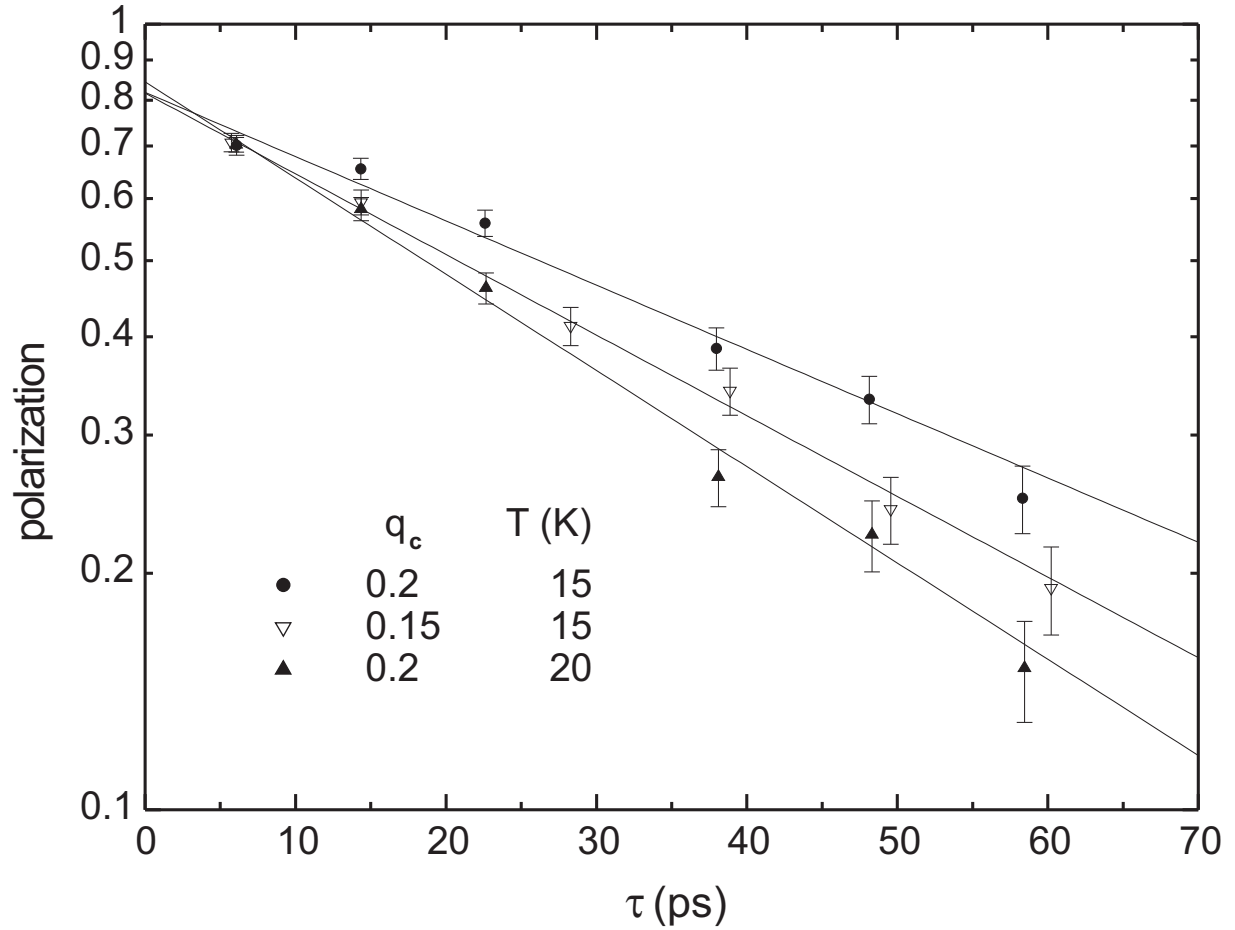


Figure 2: Raw polarization data taken at (uppermost data)  $q_c = 0.2$  r.l.u. and  $T = 15$  K, (middle)  $q_c = 0.15$  r.l.u. and  $T = 15$  K, and (lowest)  $q_c = 0.2$  r.l.u. and  $T = 20$  K. The lines are exponential fits to the data. The corresponding Lorentzian magnon linewidths (HWHM) are  $12.4 \pm 0.8$  eV,  $15.6 \pm 0.9$  eV, and  $18.6 \pm 1.0$  eV, respectively.

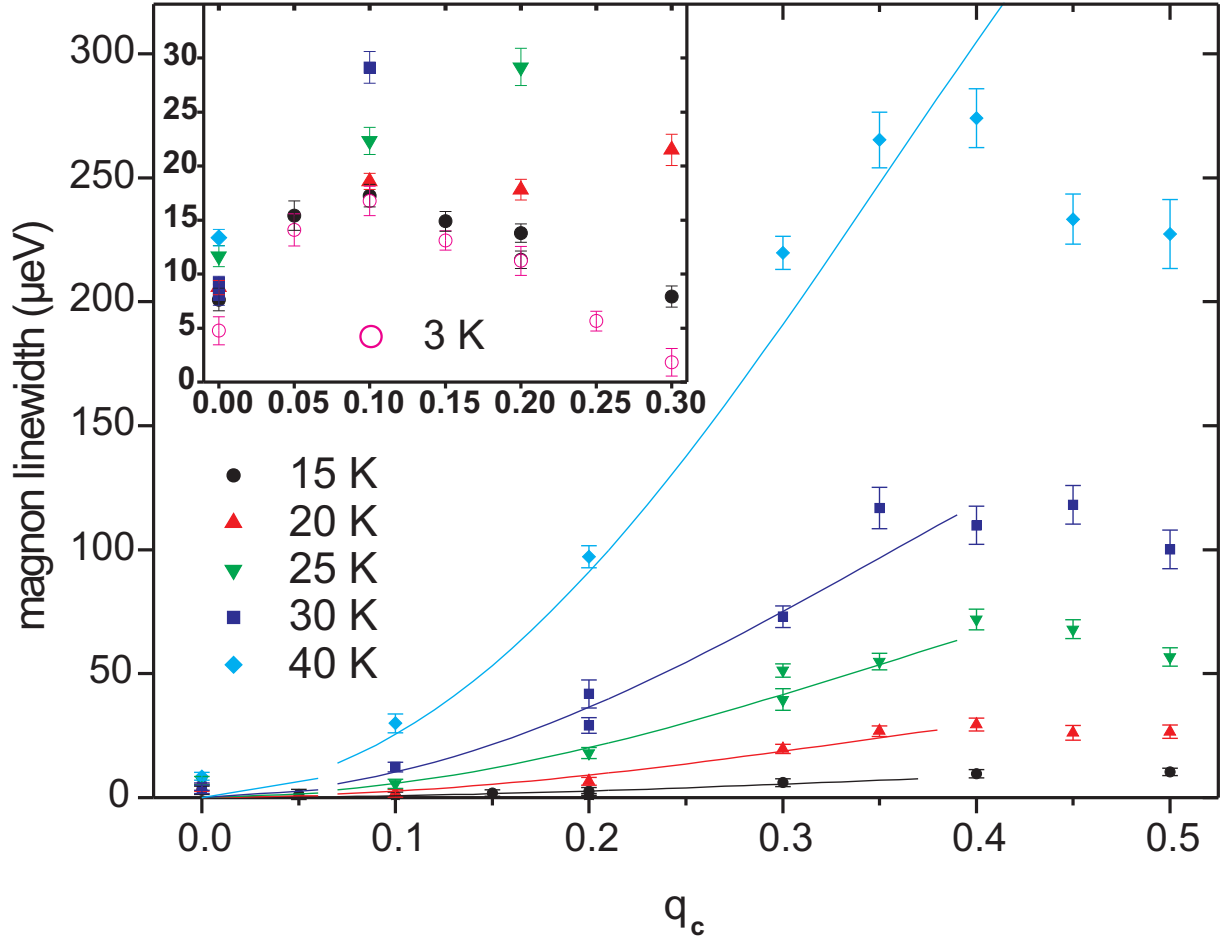


Figure 3: Intrinsic magnon linewidth  $LW$  at temperatures ranging from 15 - 40 K, as a function of  $q_c$ . We have plotted  $(LW(T, q_c) - LW(3 \text{ K}, q_c))$ , where  $LW(3 \text{ K}, q_c)$  is given in the inset (see text). The curves show theoretical expressions from Refs. [14] and [15] (see text). Two different theoretical expressions are valid for the small- $q_c$  case, depending on the magnitude of  $q_c$  relative to the anisotropy energy. Both expressions apply only to small  $q_c$ ; Stinchcombe and Reinecke have applied one of them to data extending up to  $q_c = 0.2$  r.l.u. for  $\text{MnF}_2$  near  $T_N$  [15]. However, except at  $q_c = 0$ , the theory provides an excellent fit to the data as a function of  $q_c$  up to  $q_c = 0.35$  r.l.u., both in the magnitude and in the  $q_c$ -dependence.

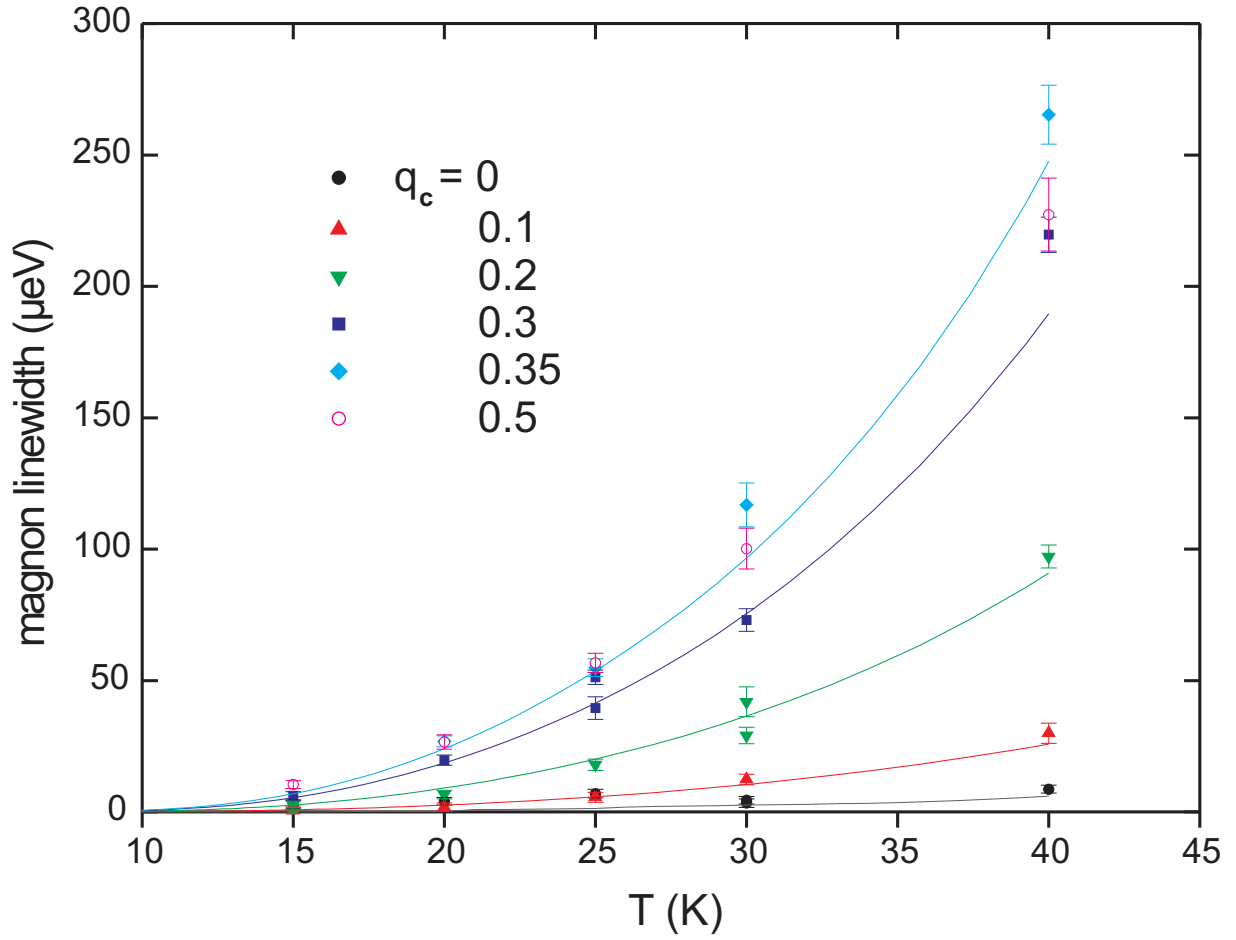


Figure 4: Intrinsic magnon linewidth with  $0 \leq q_c \leq 0.35$  r.l.u. and  $q_c = 0.5$  r.l.u., shown as a function of temperature. As in Fig. 3, data taken at 3 K has been subtracted. For  $0.1 \leq q_c \leq 0.35$  r.l.u., the curves show theoretical results from Ref. [15]. For  $q_c = 0$ , results from Harris *et al.* are plotted [12].